Long-range ferromagnetic correlations between Anderson impurities in a semiconductor host: Quantum Monte Carlo simulations

Nejat Bulut,[1,2] Kazuo Tanikawa,[1] Saburo Takahashi,[1] and Sadamichi Maekawa[1,2]
[1]*Institute for Materials Research, Tohoku University, Sendai 980-8577, Japan*
[2]*CREST, Japan Science and Technology Agency (JST), Kawaguchi, Saitama 332-0012, Japan*
(Received 23 April 2007; published 26 July 2007)

We study the two-impurity Anderson model for a semiconductor host using the quantum Monte Carlo technique. We find that the impurity spins exhibit ferromagnetic correlations with a range which can be much more enhanced than in a half-filled metallic band. In particular, the range is longest when the Fermi level is located above the top of the valence band and decreases as the impurity bound state becomes occupied. Comparisons with the photoemission and optical absorption experiments suggest that this model captures the basic electronic structure of $Ga_{1-x}Mn_xAs$, the prototypical dilute magnetic semiconductor (DMS). These numerical results might also be useful for synthesizing DMS or dilute oxide ferromagnets with higher Curie temperatures.

DOI: 10.1103/PhysRevB.76.045220 PACS number(s): 75.50.Pp, 71.55.−i, 75.30.Hx, 75.40.Mg

I. INTRODUCTION

The discovery of ferromagnetism in alloys of III-V semiconductors with Mn started an intense research activity in the field of dilute magnetic semiconductors (DMSs).[1–3] Room-temperature ferromagnetism in DMS would be a significant development for spintronics device applications. In this respect, it is important to understand the nature of the correlations which develop between magnetic impurities in semiconductors and how they differ from that in a metallic host. With this purpose, we present exact numerical results on the two-impurity Anderson model for a semiconductor host.

In order to study the multiple charge states of Au impurities in Ge, the single-impurity Anderson model of a metallic host was extended to the case of a semiconductor host using the Hartree-Fock (HF) approximation.[4] After the discovery of DMS, the magnetic properties of this model were addressed within HF.[5,6] It was shown that long-range ferromagnetic (FM) correlations develop between Anderson impurities in a semiconductor when the Fermi level is located between the top of the valence band and the impurity bound state (IBS), as illustrated in Fig. 1. The FM interaction between the impurities is mediated by the impurity-induced polarization of the valence electron spins, which are antiferromagnetically coupled to the impurity moments. The impurity-host hybridization also induces host split-off states at the same energy as the IBS. When the split-off state becomes occupied, the spin polarizations of the valence band and those of the split-off state cancel. This causes the long-range FM correlations between the impurities to vanish. Within the context of DMS, the Anderson Hamiltonian for a semiconductor host was also considered by Krstajić *et al.*,[7] and it was shown that an FM interaction is generated between the impurities due to kinematic exchange. In addition, this model was studied within HF for investigating the multiple charge and spin states of transition-metal atoms in hemoprotein.[8] Finally, the role of IBS in producing the FM interaction in DMS was also discussed within the "double resonance mechanism" using HF.[9]

In this paper, we present quantum Monte Carlo (QMC) data on the two-impurity Anderson model for a semiconductor host and make comparisons with the HF results. We find that in a semiconductor, the nature of the magnetic correlations between the impurities is different than in a metallic host. In particular, the impurities exhibit long-range FM correlations when the Fermi level is located above the top of the valence band, and the FM correlations weaken as the IBS becomes occupied, in agreement with HF.[5,6] Comparisons with the photoemission and optical absorption experiments suggest that this model captures the basic electronic structure of $Ga_{1-x}Mn_xAs$. These numerical results outline the parameter regime which yields the longest-range FM correlations, and this information might be useful for synthesizing DMS or dilute oxide ferromagnets with higher Curie temperatures.

II. MODEL

The two-impurity Anderson model for a semiconductor host is defined by

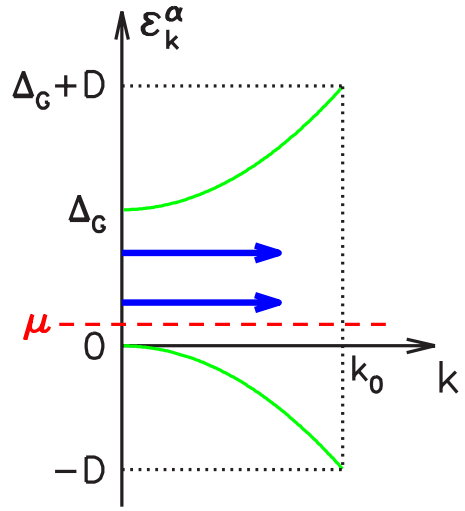

FIG. 1. (Color online) Schematic drawing of the semiconductor host bands ε_k^α (solid curves) and the impurity bound states (thick arrows) obtained with HF in the semiconductor gap. The dashed line denotes the chemical potential μ.

$$H = \sum_{\mathbf{k},\alpha,\sigma} (\varepsilon_{\mathbf{k}}^{\alpha} - \mu) c_{\mathbf{k}\alpha\sigma}^{\dagger} c_{\mathbf{k}\alpha\sigma} + \sum_{\mathbf{k},i,\alpha,\sigma} (V_{\mathbf{k}i} c_{\mathbf{k}\alpha\sigma}^{\dagger} d_{i\sigma} + \text{H.c.}) + E_d \sum_{i,\sigma} d_{i\sigma}^{\dagger} d_{i\sigma} + U \sum_{i} n_{id\uparrow} n_{id\downarrow}, \quad (1)$$

where $c_{\mathbf{k}\alpha\sigma}^{\dagger}$ ($c_{\mathbf{k}\alpha\sigma}$) creates (annihilates) a host electron with wave vector $\mathbf{k}$ and spin σ in the valence ($\alpha=v$) or conduction ($\alpha=c$) band, $d_{i\sigma}^{\dagger}$ ($d_{i\sigma}$) is the creation (annihilation) operator for a localized electron at impurity site i, and $n_{id\sigma}=d_{i\sigma}^{\dagger}d_{i\sigma}$. The hybridization matrix element is $V_{\mathbf{k}j}=V\exp(i\mathbf{k}\cdot\mathbf{R}_j)$, where $\mathbf{R}_j$ is the coordinate of the impurity site j. As usual, E_d is the d-level energy, U is the on-site Coulomb repulsion, and μ is the chemical potential. The two-site Hamiltonian, Eq. (1), was introduced for the case of metallic host in Refs. 10 and 11. Here, the valence and conduction bands have the forms $\varepsilon_{\mathbf{k}}^{v}=-D(k/k_0)^2$ and $\varepsilon_{\mathbf{k}}^{c}=D(k/k_0)^2+\Delta_G$, respectively (Fig. 1), with D the bandwidth, k_0 the maximum wave vector, and Δ_G the semiconductor gap. In this paper, we consider a two-dimensional semiconductor host with a constant density of states $\rho_0=k_0^2/(4\pi D)$. We find similar results for the three-dimensional case. The energy scale is determined by setting $D=12.0$. In addition, we use $U=4.0$ and $E_d=\mu-U/2$, so that the impurity sites develop large moments both in the metallic and semiconductor cases. We note that this Hamiltonian is particle-hole symmetric with respect to half-filling at $\mu=\Delta_G/2$. For the DMS materials, it is estimated that $\Delta_G/D\approx 0.1-0.2$. We report results for $\Delta_G=2.0$, values of the hybridization parameter $\Delta\equiv\pi\rho_0 V^2$ ranging from 1.0 to 4.0, and inverse temperature $\beta\equiv 1/T$ from 4 to 32. In order to study the evolution of the magnetic correlations as we go from a metallic to a semiconductor host, we will present results for μ from $-D/2$ to $\Delta_G/2$.

III. NUMERICAL RESULTS

The numerical results presented here were obtained with the Hirsch-Fye quantum Monte Carlo technique.[12] In the following, we will first present results on the impurity equal-time magnetic correlation function $\langle M_1^z M_2^z\rangle$, where $M_i^z=n_{id\uparrow}-n_{id\downarrow}$ is the impurity magnetization operator. Next, we will present results on the impurity single-particle spectral weight $A(\omega)=-(1/\pi)\text{Im}\, G_{ii}^{\sigma}(\omega)$, which is obtained with the maximum-entropy analytic-continuation technique[13] from the QMC data on the impurity Green's function,

$$G_{ii}^{\sigma}(\tau) = -\langle T_\tau d_{i\sigma}(\tau) d_{i\sigma}^{\dagger}(0)\rangle. \quad (2)$$

Here, T_τ is the Matsubara time-ordering operator and $d_{i\sigma}(\tau)=e^{H\tau}d_{i\sigma}e^{-H\tau}$. Since the maximum-entropy procedure requires QMC data with very good statistics, our results on $A(\omega)$ will be limited to the high-temperature $\beta=8$ case. For lower T, we will discuss QMC results on the impurity occupation number $\langle n_d\rangle=\langle n_{id\uparrow}\rangle+\langle n_{id\downarrow}\rangle$. We will also show data on the zero-frequency interimpurity magnetic susceptibility defined by

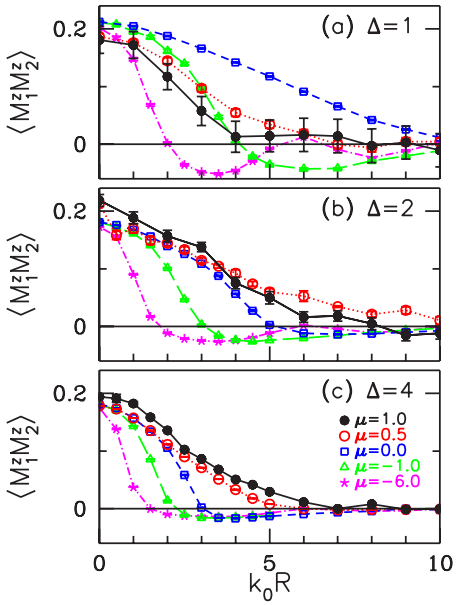

FIG. 2. (Color online) $\langle M_1^z M_2^z\rangle$ vs k_0R plotted at $\beta=16$ and various μ for hybridization $\Delta=$(a) 1.0, (b) 2.0, and (c) 4.0.

$$\chi_{12}(\omega=0) = \int_0^{\beta} d\tau \langle M_1(\tau) M_2(0)\rangle. \quad (3)$$

The following results were obtained using Matsubara time step $\Delta\tau=0.25$ except for $A(\omega)$ which was obtained with $\Delta\tau=0.125$. At $\beta=16$, $\langle M_1^z M_2^z\rangle$ varies by a few percent as $\Delta\tau$ decreases from 0.25 to 0.125. These data were obtained with more than 10^5 Monte Carlo sweeps.

Figures 2(a)–2(c) show the impurity magnetic correlation function $\langle M_1^z M_2^z\rangle$ vs k_0R, where $R=|\mathbf{R}_1-\mathbf{R}_2|$ is the impurity separation, at $\beta=16$ for μ varying from -6.0 to 1.0. Figure 2(a) is for hybridization $\Delta=1.0$. At $\mu=-6.0$, we observe oscillations in the R dependence due to a Ruderman-Kittel-Kasuya-Yoshida (RKKY)-type effective interaction between the impurities. These results are similar to what has been obtained previously with QMC for a half-filled metallic band.[12,14,15] The wavelength of the oscillations increases when μ moves to -1.0, because of the shortening of the Fermi wave vector. When $\mu=0.0$, the impurity spins exhibit long-range FM correlations at this temperature. We observe that upon further increasing of μ to 0.5 or 1.0, the FM correlations become weaker. This is because the IBS becomes occupied as μ changes from 0.0 to 0.5, as will be seen in Fig. 3(a). In Figs. 2(b) and 2(c), results on $\langle M_1^z M_2^z\rangle$ are shown for $\Delta=2.0$ and 4.0, respectively. In Fig. 2(b), we observe that $\langle M_1^z M_2^z\rangle$ has the slowest decay for $\mu=0.5$, while in Fig. 2(c), this occurs for $\mu=1.0$. We find that the impurity occupation $\langle n_d\rangle$ increases between $\mu=0.5$ and 1.0 for $\Delta=2.0$ and $\beta=16$. In addition, for $\Delta=4.0$ and $\beta=8$, the maximum-entropy image of $A(\omega)$ shows that the IBS is located at $\omega\approx 1.0$. Hence, we observe that the range of the FM correlations for the semiconductor is determined by the occupation of the IBS, in agreement with the HF predictions.[5,6] In Figs. 2(a)–2(c), it is also seen that the range increases with decreasing Δ.

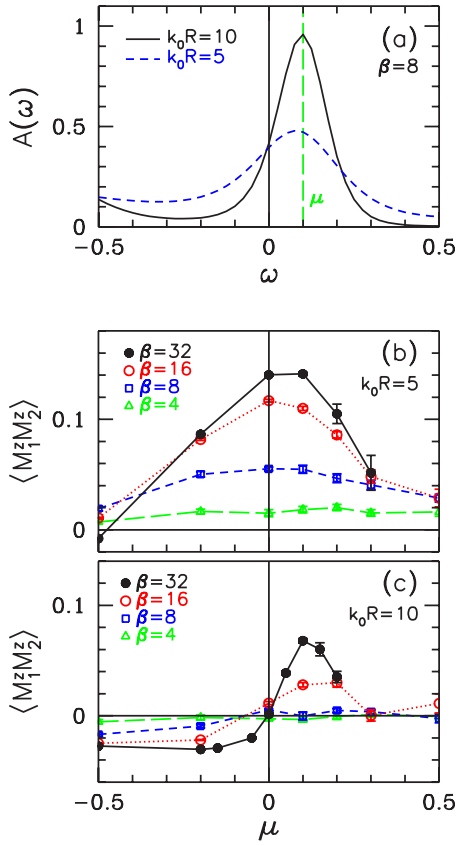

FIG. 3. (Color online) (a) Impurity single-particle spectral weight $A(\omega)$ vs ω for $k_0R=5$ and 10 at $\beta=8$. Here, the vertical dashed line denotes μ, and the top of the valence band is located at $\omega=0$. In (b) and (c), $\langle M_1^z M_2^z\rangle$ vs μ is plotted for $k_0R=5$ and 10, respectively, at various β. These results are for $\Delta=1.0$.

In Figs. 3 and 4, we discuss the $\Delta=1.0$ case in more detail. In Fig. 3(a), the impurity spectral weight $A(\omega)$ vs ω is plotted for $\beta=8$, $\mu=0.1$, and $k_0R=5$ and 10. Here, the ω axis has been shifted so that the top of the valence band is located at $\omega=0$. For $k_0R=10$, we observe a peak at $\omega_{BS}\approx 0.1$ in the semiconductor gap, which we identify as the IBS. For $k_0R=5$, the bound state is broader due to stronger correlations between the impurities. However, we also find that $A(\omega)$ exhibits significant T dependence at $\beta=8$, and Fig. 3(a) does not represent the low-T limit yet. Next, in Figs. 3(b) and 3(c), $\langle M_1^z M_2^z\rangle$ evaluated at $k_0R=5$ and 10 is plotted as a function of μ. Figure 3(b) shows that, at low T for $k_0R=5$, $\langle M_1^z M_2^z\rangle$ decreases when $\mu\gtrsim 0.25$. For this value of k_0R and $\beta=32$, we find that the impurity occupation $\langle n_d\rangle$ develops a step discontinuity at $\mu\approx 0.25$, which is consistent with the decrease of $\langle M_1^z M_2^z\rangle$ when $\mu\gtrsim 0.25$. For $k_0R=10$ and $\beta=32$, both $\langle M_1^z M_2^z\rangle$ and $\langle n_d\rangle$ exhibit significant T dependence in the vicinity of the semiconductor gap edge. These results show that $\langle M_1^z M_2^z\rangle$ depends strongly on the value of μ.

Figure 4(a) shows the temperature dependence of $\langle M_1^z M_2^z\rangle$ vs k_0R for $\mu=0.1$. We observe that, at $\beta=32$, the range of the FM correlations is enhanced by about an order of magnitude with respect to that in a half-filled metallic band. In Fig. 4(b), the T dependence of the interimpurity susceptibility $\chi_{12}(\omega=0)$ is shown for $k_0R=10$ and various values of μ. We observe that, as β increases, χ_{12} becomes strongly enhanced for $\mu=0.1$, while it remains weak for $\mu=0.3$. At $\mu=-0.2$, χ_{12} is antiferromagnetic for this value of k_0R. Figures 3 and 4 show that long-range FM correlations develop between the impurities depending on the position of μ.

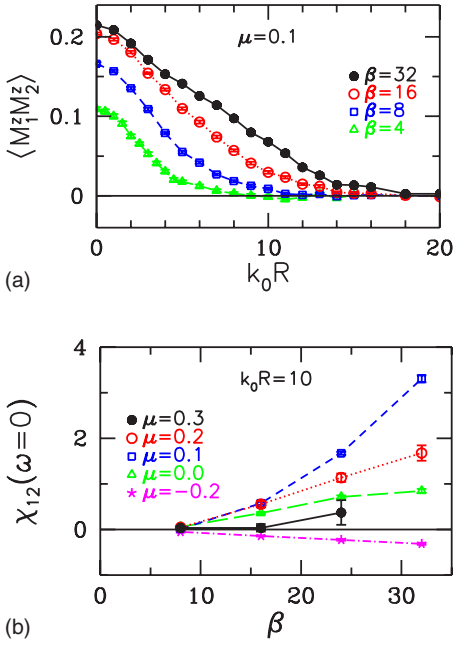

FIG. 4. (Color online) (a) $\langle M_1^z M_2^z\rangle$ vs k_0R for $\mu=0.1$ at various β. (b) Interimpurity magnetic susceptibility $\chi_{12}(\omega=0)$ vs β for $k_0R=10$ at various μ. These results are for $\Delta=1.0$.

In the QMC simulations, we find that $\langle M_1^z M_2^z\rangle$ has larger error bars when IBS is occupied. This might be due to the cancellation of the host spin polarizations originating from the split-off state and from the valence band. The intraimpurity measurements such as $\langle (M_1^z)^2\rangle$ or $G_{ii}^{\sigma}(\tau)$ do not exhibit such behavior.

Within HF, the range ξ of the FM correlations between the impurities is determined by the energy of the IBS and, hence the energy of the split-off state: $\xi\approx(16\pi\rho_0\omega_{BS})^{-1/2}$ for a constant density of states and semi-infinite host bands. In particular, the spatial extent of the spin polarization of the valence band around the impurity is given by $4\rho_0\Delta Z_d e^{-r/\xi}/(r/\xi)$, where Z_d is the weight of the pole at ω_{BS} in the impurity single-particle Green's function. Within HF, ω_{BS} decreases rapidly as $\Delta/\Delta_G\to 0$, which agrees with the Δ dependence of the range seen in Figs. 2(a)–2(c). In addition, for $T=0$, $\Delta=1.0$, and $0<\mu<\omega_{BS}$, HF yields $\omega_{BS}\approx 0.02$ and $k_0\xi\approx 9$. Hence, while the HF yields a ξ in agreement with QMC, the result for ω_{BS} is much smaller. Consequently, within HF, the long-range FM correlations are restricted to a narrow range of μ. This is the main difference we find between QMC and HF, and it is probably because the effects of the interimpurity correlations on the single-particle Green's functions are neglected within HF.

IV. DISCUSSION

In the QMC and HF calculations, the location of the Fermi level with respect to the IBS is important; the FM

correlations weaken as the IBS becomes occupied. Photoemission and optical measurements on $Ga_{1-x}Mn_xAs$ provide evidence that the occupation of the Mn-induced impurity band is similarly important for the magnetic properties of this prototypical DMS ferromagnet. Photoemission experiments[16] observed a Mn-induced state above the valence band and right below the Fermi level in $Ga_{1-x}Mn_xAs$. Clearly, inverse photoemission experiments are required to detect the unoccupied portion of the Mn-induced impurity band. Scanning tunneling microscopy experiments also observed the impurity band in this compound.[17] Recent optical-absorption measurements,[18] which show a redshift of the midinfrared peak with Mn doping, provide evidence that the Fermi level is located in the Mn-induced impurity band in $Ga_{1-x}Mn_xAs$. Furthermore, as the impurity band becomes less occupied with Mn doping, the Curie temperature T_c increases in annealed samples, which is in agreement with the QMC and HF results. The comparisons of these experiments and the numerical results suggest that the Anderson Hamiltonian for a semiconductor host provides a basic electronic model for the DMS ferromagnets.

Alternative ways of enhancing the FM correlations in this model are provided by varying the hybridization parameter Δ or the semiconductor gap Δ_G. The QMC simulations show that ξ increases as Δ goes from 4.0 to 1.0. Within HF, ξ can take very large values as Δ/Δ_G decreases. Hence, new DMS compounds with weaker hybridization or a larger semiconductor gap might lead to higher Curie temperatures. However, it is necessary to keep in mind that the two-impurity Anderson model for a semiconductor host might be oversimplified for describing the ferromagnetism of the DMS. Our calculations are for spin-1/2 Anderson impurities, and we have neglected the multiorbital structure of the spin-5/2 Mn impurities. Hence, the effects of the atomic Hund's rule couplings are not included. In addition, we neglect the long-range Coulomb repulsion between the impurity and the host electrons. Furthermore, we have used a simple band structure for the semiconductor host. These are the main limitations of our calculations.

Various other theoretical approaches have been used to describe the ferromagnetism of DMS and to predict the Curie temperature as a function of the Mn concentration. These include the coherent potential approximation (CPA) and local density approximation (LDA)$+U$ techniques which describe the host band structure more accurately but treat the Coulomb correlations approximately.[19] In particular, we note that the CPA- or LDA$+U$-type calculations cannot be relied upon to accurately predict the dependence of the FM correlations on μ or Δ/Δ_G. In this respect, the results presented in this paper are valuable because here, the many-body effects due to the Coulomb correlations at the impurity site in a semiconductor host have been treated exactly. For example, we have observed that, within the HF approximation, the long-range FM correlations are restricted to a narrow range of μ. We also point out that the dependence of the Curie temperature on the carrier concentration has been studied for DMS using a disordered RKKY model.[20] However, our results show that the RKKY form is not appropriate for describing the interimpurity magnetic correlations when the host is a semiconductor. In the future, we plan to calculate the effective impurity-host and impurity-impurity magnetic-exchange couplings using QMC for the same Hamiltonian.

Recently, T_c's exceeding the room temperature have been reported in dilute oxides such as ZnO and TiO_2 with transition-metal impurities.[21,22] The importance of the oxygen vacancies in producing the ferromagnetism has been pointed out experimentally.[23] Perturbative and LSDA$+U$ mean-field calculations have been performed to describe the ferromagnetism induced by oxygen vacancies in $(Ti,Co)O_2$.[24,25] We think that it would also be useful to perform exact numerical calculations to study the role of the vacancy band in producing the FM correlations in this compound.

V. SUMMARY

In summary, we have presented QMC results to show that long-range FM correlations develop between magnetic impurities in semiconductors. In particular, the FM correlations have the longest range when the Fermi level is located above the top of the valence band, and they weaken as the IBS becomes occupied. Hence, the position of the Fermi level with respect to the IBS plays a crucial role in determining the range of the FM correlations, in qualitative agreement with HF. Comparisons with the photoemission and optical absorption experiments suggest that the two-impurity Anderson model in a semiconductor host captures the basic electronic structure of $Ga_{1-x}Mn_xAs$. The numerical results presented here outline the parameter regime which yields the longest-range FM correlations, and this information might be useful for synthesizing higher-T_c DMS materials.

ACKNOWLEDGMENTS

We thank V. A. Ivanov for bringing Ref. 7 to our attention and for useful comments. This work was supported by the NAREGI Nanoscience Project and a Grant-in Aid for Scientific Research from the Ministry of Education, Culture, Sports, Science and Technology of Japan, and NEDO. One of us (N.B.) gratefully acknowledges support from the Japan Society for the Promotion of Science and the Turkish Academy of Sciences (EA-TUBA-GEBIP/2001/1-1).

[1] *Concepts in Spin Electronics*, edited by S. Maekawa (Oxford University Press, New York, 2006).

[2] H. Ohno, H. Munekata, T. Penney, S. von Molnar, and L. L. Chang, Phys. Rev. Lett. **68**, 2664 (1992); H. Ohno, A. Shen, F. Matsukura, A. Oiwa, A. End, S. Katsumoto, and Y. Iye, Appl. Phys. Lett. **69**, 363 (1996).

[3] I. Žutić, J. Fabian, and S. Das Sarma, Rev. Mod. Phys. **76**, 323 (2004).

[4] F. D. M. Haldane and P. W. Anderson, Phys. Rev. B **13**, 2553 (1976).
[5] M. Ichimura, K. Tanikawa, S. Takahashi, G. Baskaran, and S. Maekawa, *Foundations of Quantum Mechanics in the Light of New Technology (ISOM-Tokyo 2005)*, edited by S. Ishioka and K. Fujikawa (World Scientific, Singapore, 2006), pp. 183–186.
[6] K. Tanikawa, S. Takahashi, M. Ichimura, G. Baskaran, and S. Maekawa (unpublished).
[7] P. M. Krstajić, V. A. Ivanov, F. M. Peeters, V. Fleurov, and K. Kikoin, Europhys. Lett. **61**, 235 (2003).
[8] K. Yamauchi, H. Maebashi, and H. Katayama-Yoshida, J. Phys. Soc. Jpn. **72**, 2029 (2003).
[9] J. Inoue, S. Nonoyama, and H. Itoh, Phys. Rev. Lett. **85**, 4610 (2000).
[10] S. Alexander and P. W. Anderson, Phys. Rev. **133**, A1594 (1964).
[11] B. Caroli, J. Phys. Chem. Solids **28**, 1427 (1967).
[12] J. E. Hirsch and R. M. Fye, Phys. Rev. Lett. **56**, 2521 (1986).
[13] W. von der Linden, Appl. Phys. A: Mater. Sci. Process. **60**, 155 (1995).
[14] R. M. Fye, J. E. Hirsch, and D. J. Scalapino, Phys. Rev. B **35**, 4901 (1987).
[15] R. M. Fye and J. E. Hirsch, Phys. Rev. B **38**, 433 (1988).
[16] J. Okabayashi, A. Kimura, O. Rader, T. Mizokawa, A. Fujimori, T. Hayashi, and M. Tanaka, Phys. Rev. B **64**, 125304 (2001).
[17] A. M. Yakunin, A. Yu. Silov, P. M. Koenraad, J. H. Wolter, W. Van Roy, J. De Boeck, J.-M. Tang, and M. E. Flatte, Phys. Rev. Lett. **92**, 216806 (2004).
[18] K. S. Burch, D. B. Shrekenhamer, E. J. Singley, J. Stephens, B. L. Sheu, R. K. Kawakami, P. Schiffer, N. Samarth, D. D. Awschalom, and D. N. Basov, Phys. Rev. Lett. **97**, 087208 (2006).
[19] T. Jungwirth, J. Sinova, J. Masek, J. Kucera, and A. H. MacDonald, Rev. Mod. Phys. **78**, 809 (2006).
[20] D. J. Priour and S. Das Sarma, Phys. Rev. Lett. **97**, 127201 (2006).
[21] Y. Matsumoto, M. Murakami, T. Shono, T. Hasegawa, T. Fukumura, M. Kawasaki, P. Ahmet, T. Chikyow, S. Koshihara, and H. Koinuma, Science **291**, 854 (2001).
[22] P. Sharma, A. Gupta, K. V. Rao, F. J. Owens, R. Sharma, R. Ahuja, J. M. O. Guillen, B. Johansson, and G. A. Gehring, Nat. Mater. **2**, 673 (2003).
[23] K. A. Griffin, A. B. Pakhomov, C. M. Wang, S. M. Heald, and K. M. Krishnan, Phys. Rev. Lett. **94**, 157204 (2005).
[24] K. Kikoin and V. Fleurov, Phys. Rev. B **74**, 174407 (2006).
[25] V. I. Anisimov, M. A. Korotin, I. A. Nekrasov, A. S. Mylnikova, A. V. Lukoyanov, J. L. Wang, and Z. Zeng, J. Phys.: Condens. Matter **18**, 1695 (2006).